Proc. 21st Winter Workshop on Nuclear Dynamics (2005) 000–000

21st Winter Workshop on Nuclear Dynamics
Breckenridge, Colorado, USA
February 5–12, 2005

Hadron Production at Forward and Backward Rapidities in $\sqrt{s_{NN}} = 200$ GeV d+Au Collisions

Andrew Glenn[1] for the PHENIX Collaboration

[1] University of Colorado, Boulder
Boulder, CO 80309, USA

Abstract. Understanding normal nuclear medium effects present in heavy ion collisions is essential for understanding the following dynamics of the high density matter produced in the collision. Asymmetric collisions, such as deuteron + gold, provide a key tool for studying these effects since particles produced in the forward and backward directions may be subject to different phenomena. Particle production has been studied in d+Au collisions for various kinematic regions at the RHIC facility. PHENIX has measured charged hadron production as a function of p_T for different centrality classes using the PHENIX muon spectrometers for d+Au collisions at $\sqrt{s_{NN}} = 200$ GeV. The PHENIX muon spectrometers have coverage in both forward and backward directions in the rapidity range $1.2 < |\eta| < 2.4$. The R_{cp} measurement, the ratio of central to peripheral production, is presented and discussed. Comparisons are also made with some relevant theoretical calculations.

Keywords: Nuclear modification factor, relativistic heavy ion collisions
PACS: 25.75.-q

1. Introduction

A strong increase in the gluon density of the proton's Parton Distribution Functions is seen at high Q^2 and small x, fraction of the proton momentum carried by the parton, from the DGLAP and BFKL evolution equations [1]. Such an increase is observed at HERA in quark and antiquark distribution functions [2], implying that at sufficiently small x, gluons may overlap in space and time. This overlap may cause increased gluon fusion; reducing the gluon density at low x and enhancing the density at larger x. The low x gluon fusion limits the maximum gluon density causing gluon saturation. One description of such a saturation is the Color Glass Condensate (CGC) [3] model. Gluon saturation is expected to be larger in nuclei

since the partons from different nucleons overlap.

Gluon saturation at small x, corresponding to forward rapidities through $x = \frac{M_T}{\sqrt{s}}e^{-y}$, has been predicted to suppress hadronic yields [4] for $d + Au$ collisions at RHIC energies, where Q_s^2 is expected to be around $2 - 4$ GeV^2. However, other hadron production mechanisms, such as quark recombination [5], can also result in an effective suppression in the forward rapidity region. Results on charged hadron yields at forward rapidity from the BRAHMS experiment have shown a suppression of the yield of hadrons in central, compared to peripheral, $d + Au$ collisions [6].

2. Experimental Setup and Analysis Details

PHENIX includes two spectrometers designed for measuring muon production over the pseudorapidity ranges $-2.2 < \eta < -1.2$ (backward spectrometer) and $1.2 < \eta < 2.4$ (forward spectrometer) [7]. The spectrometers use a thick hadron absorber comprised of 19 cm of brass and 60 cm of low-carbon steel between the collision point and active detectors along the beam axis to reduce hadronic background for muon measurements [8]. Beyond the absorbers, the Muon Tracker (MuTr) detector, consisting of three stations of cathode strip chambers, tracks charged particles in a magnetic field. The momentum resolution is 5% for typical momenta in this analysis, and the absolute scale is known to better than 1%.

A Muon Identifier (MuID) is located after the muon magnet backplate of 30 (20) cm of steel in the forward (backward) spectrometer. The MuID consists of five layers of planar drift tubes interleaved with 10 cm thick plates of steel for the first two layers and 20 cm thick plates for the remaining layers for further hadron absorption. The layers are numbered 0-4, with 4 being farthest from the collision vertex. The MuID is used to help separate muons from hadrons and provide triggering capabilities.

Two different trigger configurations were used to collect data sets for this analysis. The first data set contained 67×10^6 minimum bias triggers, which require at least one hit in both the PHENIX forward $3.0 < \eta < 3.9$ and backward $-3.9 < \eta < -3.0$ Beam-Beam Counters (BBC) and a reconstructed vertex position within $|z| < 30$ cm along the beam axis, were recorded. The minimum bias trigger accepts $88 \pm 4\%$ of all inelastic $d + Au$ collisions [9]. The second data set, sampling 5.3×10^9 minimum bias events, was collected using a MuID trigger which requires at least one track penetrating the first four layers of the MuID.

The events are divided into four centrality classes based on the number of particle hits in the backward (Au beam direction) BBC counter, which covers $-3.9 < \eta < -3.0$. The average number of binary collisions in each centrality class is determined using a Glauber model [9] and simulation of the BBC. The classes are categorized as follows: $60-88\%$ ($\langle N_{coll} \rangle = 3.1 \pm 0.3$), $40-60\%$ ($\langle N_{coll} \rangle = 7.0 \pm 0.6$), $20 - 40\%$ ($\langle N_{coll} \rangle = 10.6 \pm 0.7$),and $0 - 20\%$ ($\langle N_{coll} \rangle = 15.4 \pm 1.0$).

There is a correlation between having a particular physics process, the production of a high p_T hadron for example, and the BBC response. The BBC coverage

in pseudorapidity is well separated from that of the muon spectrometers, so the correlation is primarily due to an underlying event correlation rather than jet fragmentation. Proton-proton, $d+Au$, and simulated data have been used to study in detail and account for the effect of this correlation bias. The applied bias correction factors range from 0-7% depending on the centrality category and the physics process. The systematic errors on these corrections are less than 4%.

Although the forward and backward spectrometers were designed to detect muons, they can also be used for charged hadrons measurements. Both muons and hadrons lose energy via ionization when passing through material. Hadrons can also experience strong nuclear interactions which substantially reduce their ability to penetrate through the spectrometer.

2.1. Punch-through hadrons

The punch-through hadron identification is achieved by studying particles that stop within the MuID before the last layer. For muons penetrating up to layer 2 and 3 we expect the average momenta measured in the MuTr of $p = 1.0\,\mathrm{GeV}/c$ and $p = 1.2\,\mathrm{GeV}/c$, respectively. The reconstructed momentum distributions for particles stopping in layers 2 and 3 of the MuID are shown in Figure 1. In addition to

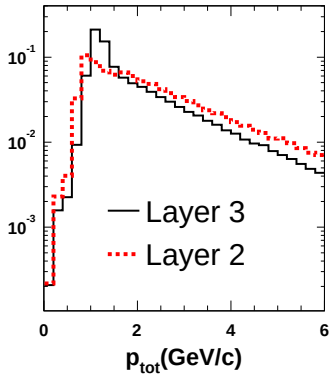

Fig. 1. (color online). The total momentum p_{tot} measured in the MuTr without energy loss correction of all charged tracks penetrating to MuID layers 2 and 3.

the expected muon peaks, there is a broad distribution extending to higher momentum which is the result of punch-through hadrons. These hadrons suffer ionization energy loss, similarly to muons, up to the relevant layer and then suffer a hadronic interaction in the MuID steel which stops the penetration. This allows for selection of a clean sample of hadrons by demanding that a track stop in MuID layer 2 or 3 and have momentum more than 3σ away from the muon peaks. Muon contamination in the sample is estimated from simulations to be less than 5%.

2.2. Muons from Hadron Decays

Some hadrons will decay into muons before the absorber, and the decay muons are then measured by the muon spectrometers. Muons can result from many sources including decays of π, K, D mesons, and J/ψ. These particles have a finite decay probability P_{decay} before they reach the absorber

$$P_{decay}(p, L) = 1 - e^{-\frac{L \cdot m}{\tau \cdot p}} \tag{1}$$

where $L \sim 41$cm, is the distance from the collision vertex to the absorber; p, m and τ are the momentum, mass and proper lifetime of the parent particle.

This causes collisions which occur far from the absorber to be more likely to produce muons from light meson decays than those which occur close to the absorber. In contrast, charmed hadrons, due to their very short proper decay lengths, $e^{-\frac{L \cdot m}{\tau \cdot p}} \ll 1$, will have a negligible collision vertex dependence. Figure 2 shows the collision vertex distribution for events in which muons are detected at forward rapidity, corrected for the non-flat minimum bias collision vertex distribution. The

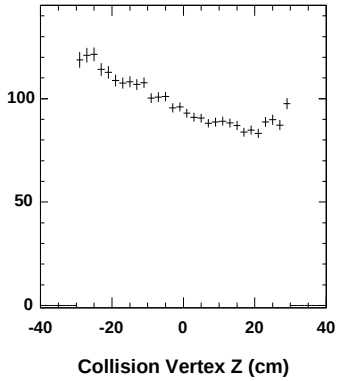

Fig. 2. Collision vertex distribution for events with muons at forward rapidity, corrected for the minimum bias collision vertex distribution.

large vertex dependence indicates a significant fraction of the muons are from pion and kaon decays. This distribution can be used to separate the decay muons from pions and kaons from other contributions. The measured muon p_T used in the analysis is approximately 15% lower on average than the parent hadron p_T.

3. Results and Comparisions

The *nuclear modification factor* R_{cp} is defined as the ratio of the particle yield in central collisions to the particle yield in peripheral collisions, each normalized by

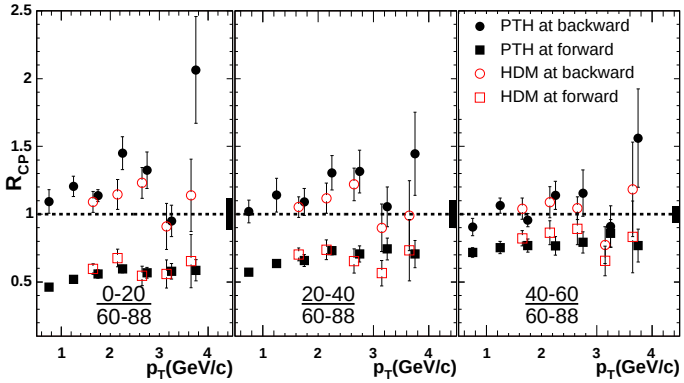

Fig. 3. (color online). R_{cp} as a function of p_T at forward rapidity (squares) and backward rapidity (circles) for different centrality classes.

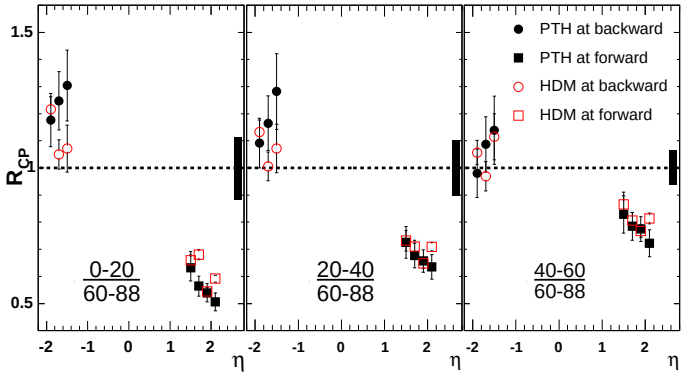

Fig. 4. (color online). R_{cp} as a function of η for $1.5 < p_T < 4.0\,\mathrm{GeV}/c$ for different centrality classes.

the average number of nucleon-nucleon binary collisions ($\langle N_{coll}\rangle$):

$$R_{cp} = \frac{\langle\left(\frac{dN}{d\eta dp_T}\right)^{Central}\rangle/\langle N_{coll}^{Central}\rangle}{\langle\left(\frac{dN}{d\eta dp_T}\right)^{Peripheral}\rangle/\langle N_{coll}^{Peripheral}\rangle} \tag{2}$$

The hadron R_{cp}, using the most peripheral centrality class $(60-88\%)$ for normalization, is shown in Figure 3 as a function of p_T at forward and backward rapidities. The results from both the punch-through hadron (PTH) and hadron decay muon (HDM) analyses are shown and are in good agreement. Figure 4 shows the results integrated over $1.5 < p_T < 4.0\,\mathrm{GeV}/c$ as a function of pseudorapidity. Systematic uncertainties which move all data points up and down are shown as a black bar at

$R_{cp} = 1$. The quadratic sum of point to point systematic and statistical errors are shown as error bars.

One noteworthy difference is that the two measurement methods have different sensitivity to different hadrons. The measured particle composition ($\pi/K/p$ ratio) is modified relative to the particle composition at the collision vertex due to species-dependent nuclear interaction cross-sections, which affect the punch-through hadrons, and species-dependent decay lifetimes, which affect the hadron decay muons. Both effects enhance the kaon contribution to our R_{cp} measurements. The uncertainty on the charged hadron R_{cp} values introduced by this effect is estimated to be less than 4% by calculating the difference between the kaon R_{cp} and inclusive charged particle R_{cp} determined by PHENIX at mid-rapidity [10].

In Figure 5 results from the BRAHMS experiment [6] are compared with the results of this analysis at forward rapidity. The PHENIX data and the BRAHMS data are in agreement within systematic uncertainties. It should be noted that

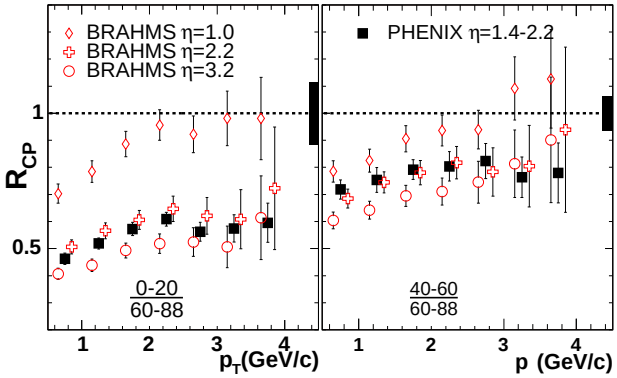

Fig. 5. (color online). PHENIX R_{cp} as a function of p_T at forward rapidities shown as the average of the two methods. Note that the BRAHMS results are for negative hadrons at $\eta = 2.2, 3.2$ and the centrality ranges ($0-20\%/60-80\%$ and $30-50\%/60-80\%$) differ from those used in this analysis.

HIJING/GEANT studies performed by BRAHMS indicate that the particular acceptance of the Si Multiplicity Array and Tile Multiplicity array used by BRAHMS to measure centrality causes a currently uncorrected bias [11] which could impact their result. Figure 6 shows a comparison of the PHENIX measurement to a CGC model calculation [13]. The calculation shows a fair agreement with the data, but it should be noted that parameters of the model were tuned to match BRAHMS data. While a suppression at forward rapidity is expected from shadowing expectations, clear quantitative agreement has not yet been demonstrated. Figure 7 shows the PHENIX data compared to recent shadowing calculations [14]. The use of the $S_{GFS,\rho}$ shadowing function does not significantly improve the agreement.

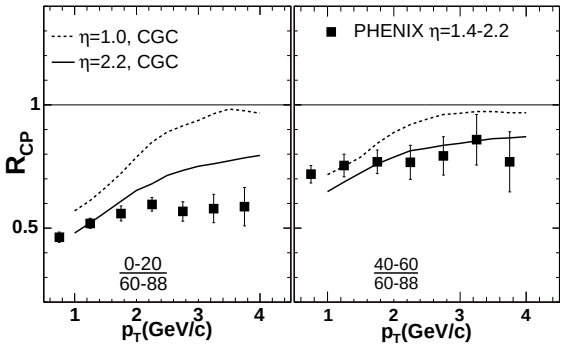

Fig. 6. Comparison [12] between a CGC model calculation [13] and the PHENIX R_{cp} for punch through hadrons.

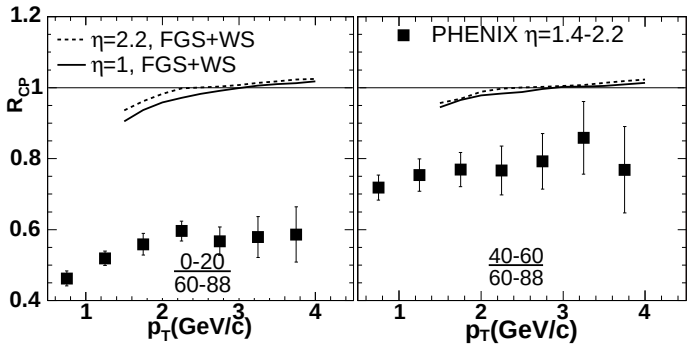

Fig. 7. Comparison [12] between FGS parameterization and the PHENIX R_{cp} for punch through hadrons. The shadowing function used in the calculation is $S_{FGS,WS}$. Note the calculation was done for the BRAHMS RCP, as we mentioned that the centrality definition were different between BRAHMS and PHENIX.

4. Conclusions

The charged hadron R_{cp} measured by PHENIX shows a suppression at forward rapidity, the deuteron going direction, which is largest for the most central events. The opposite trend is observed at backward rapidity where R_{cp} shows a slight enhancement that is also largest for the most central events. A weak p_T dependence is observed with slightly smaller R_{cp} values at lower p_T. A clear pseudorapidity dependence is present at forward rapidity with R_{cp} dropping further at larger η values. The forward rapidity R_{cp} values show fair agreement with a CGC model calculation tuned using BRAHMS data, and poor agreement with the examined shadowing calculations. Within current uncertainties, there is no discernable pseudorapidity dependence at backward rapidity.

Acknowledgments

We thank the staff of the Collider-Accelerator and Physics Departments at BNL for their vital contributions. We acknowledge support from the Department of Energy and NSF (U.S.A.), MEXT and JSPS (Japan), CNPq and FAPESP (Brazil), NSFC (China), IN2P3/CNRS, CEA, and ARMINES (France), BMBF, DAAD, and AvH (Germany), OTKA (Hungary), DAE and DST (India), ISF (Israel), KRF and CHEP (Korea), RMIST, RAS, and RMAE (Russia), VR and KAW (Sweden), U.S. CRDF for the FSU, US-Hungarian NSFOTKA- MTA, and US-Israel BSF.

References

1. G. Altarelli and G. Parisi, Nucl. Phys. **B126**, 298 (1977); Y.L. Dokshitzer, Sov. Phys. JETP **46**, 641 (1977); V.N. Gribov and L.N. Lipatov, Sov. J. Nucl. Phys. **15**, 438 (1972).
2. H. Abramowicz and A.C. Caldwell, Rev. Mod. Phys. **71**, 1275 (1999).
3. L. McLerran and R. Venugopalan, Phys. Rev. D **49**, 2233 (1994); Phys. Rev. D **49**, 3352 (1994).
4. A. Dumitru and J. Jalilian-Marian, Phys. Lett. **B547**, 15 (2002); F. Gelis and J. Jalilian-Marian, Phys. Rev. D **66**, 014021 (2002).
5. R. Hwa, C.B. Yang, R.J. Fries, arXiv:nucl-th/0410111.
6. I. Arsene *et al.*, Phys. Lett. **B595**, 209 (2004).
7. K. Adcox *et al.*, Nucl. Instrum. Methods **A499**, 469 (2003) and references therein.
8. S.H Aronson *et al.*, Nucl. Instrum. Methods **A449**, 480-488 (2003).
9. S. S. Adler *et al.*, Phys. Rev. Lett. **91**, 072303 (2003).
10. F. Matathias *et al.*, J. Phys **G30**, S1113 (2004).
11. I. Arsene *et al.* [BRAHMS Collaboration], Phys. Rev. Lett. **94**, 032301 (2005) [arXiv:nucl-ex/0401025].
12. C. Zhang, Ph.D Thesis, http://www.phenix.bnl.gov/phenix/WWW/publish/zhangc/thesis/thesis_chun.pdf
13. D. Kharzeev, Y. V. Kovchegov and K. Tuchin, Phys. Lett. B **599**, 23 (2004)
14. R. Vogt, arXiv:hep-ph/0405060.